A novel compact 4 x 4 Multi-slot MIMO antenna for N78/79, Wi-Fi 5/6, and V2X/DSRC for 5G in Sub-6 GHz band

Pendli Pradeep[1]*, K. Jaya Sankar[2], and Chandra Sekhar Paidimarry[3]

[1]Electronics and Communication Engineering, Sreenidhi Institute of Science and Technology, Hyderabad, India
[2]Electronics and Communication Engineering, Methodist College of Engineering and Technology, Hyderabad, India
[3]Electronics and Communication Engineering, University College of Engineering, Osmania University, Hyderabad, India

Corresponding author: Pendli Pradeep (e-mail: pradeeppendli@gmail.com).

ABSTRACT In this article, a novel multi-slot 2-port and 4-port compact wideband MIMO antennas are designed for 5G communication in the sub-6 GHz band. The multi-slot antenna contains a rectangular patch with two square cuts at the lower corner of it. Here, two rectangular slots, one at the top edge and the other near the bottom edge of the antenna. The orthogonal placement technique helps to provide initial isolation between ports. Further, a P-shaped stub is added to the top edge of the antenna element to achieve very high isolation among 4 antennas. The FR4 substrate's overall dimensions are considered 56 x 56 x 1.6 mm^3. The proposed 4-port multi-slot antenna achieved isolation of > 15 dB in the operating frequency band from 3.60 GHz – 7.33 GHz. The 4-port multi-slot prototype results and its simulated results are almost similar. The radiation patterns in elevation and azimuth planes are stable, a peak gain and high efficiency are 5.2 dB and 95% respectively. This antenna performance can be envisaged for N78/79, Wi-Fi 5/6, and Vehicle2X/DSRC bands.

INDEX TERMS NR 5G Sub-6 GHz, P-shaped stub, Isolation, and MIMO antenna.

I. INTRODUCTION

Due to advancements in wireless technology, 5G communication requires faster, good-quality services and high channel capacity. MIMO (Multiple Inputs and Multiple Outputs) is an incredible technique in 5G technology for wireless connectivity. MIMO antenna has very high data rate communication, low multipath fading effects, and link reliability. The unique challenge in the MIMO antenna system is to achieve very high isolation along with a compact size for portable devices. In literature, some of the works reported on single, dual, and multiband MIMO antenna systems as follows, A 4 x 4 MIMO antenna pentagonal patch antenna with slot was proposed for WLAN applications [1]. Two orthogonally spaced dual-band MIMOs are proposed to achieve a compact-size antenna along with high isolation between antenna elements [2]. A MIMO antenna with decagon-shaped rings is used as a radiator to operate in multi-band for WLAN/WiMAX/5G applications [3]. A compact pattern diversity 4 x 4 multiple antenna is presented in WLAN/WiFi/5G applications [4]. A Hammer-shaped 4 x 4 MIMO antenna is presented for WLAN applications [5]. Two port CPW MIMO antenna is presented [6], A dual-mode antenna is printed at both sides of the substrate and forms a 4 x 4 MIMO slot antenna for wireless applications [7], Wideband four port MIMO antenna [8], A four-port CPW fed monopole antenna is designed for WiMAX, WLAN, and satellite applications [9], and A square-shaped patch incorporated with circular and rectangular-shaped slots to operate in triple bands presented [10]. A Four-port common radiator as a MIMO antenna element for Wi-Fi devices [11]. Multi-cut four-port shared radiator is presented for WLAN application [12]. A two-port Compact MIMO Semi-circular Slot is proposed for NR mid-band Sub-6 GHz by enhancing isolation between antenna ports [13]. A 2-port MIMO antenna is proposed as a fractal shape antenna for lower sub-6-GHz band applications [14]. Novel bent slits are used in a MIMO antenna to achieve wider bandwidth [15]. A metasurface structure is used to present a 2-port MIMO antenna system to achieve wider bandwidth, high gain, and isolation [16]. A 2-port dual-band trident-shaped antenna system is evaluated for 5G applications [17]. A fractal v-shaped MIMO antenna design is to cover 4.7 GHz-5 GHz for 5G Smartphone applications with a copper lining to enhance isolation between antenna ports [18]. A 4-element MIMO antenna with DGS at one port is presented for Wireless LAN applications [19]. A UWB MIMO antenna is presented like loop excitation [20]. A Cow-Head shape converted as a 2-port MIMO antenna to function in the Sub:6 GHz band [21]. A 4 x 4 MIMO quad-radiating antenna is presented for LTE/Wi-Fi applications [22]. A four-port trapezoidal shaped

circularly polarized is designed on a printed circuit board as a MIMO antenna for Wi-Fi/WLAN (5 GHz), Wi-MAX, and C band applications [23]. A 2-port triple band shared ground MIMO antenna designed for ISM, and WLAN Applications [24]. A very low mutual coupling modified ground 2-port antenna is designed as a dual-band element for multiple band applications in sub-6 GHz bands [25]. SRR based MIMO antenna and MIMO antenna for cognitive radio are presented in [26-27]. CP MIMO antennas for C-band, mm-wave 5G NR n260 band, WLAN applications [28-30]. However, due to trade-offs among MIMO antenna parameters, further improvements are required in MIMO antenna systems. Our work 4-port MIMO antenna addressed and optimized with improved characteristics like compact size, high isolation, channel capacity, gain, and low mutual coupling effects.

In this article, a novel 4 port compact wideband MIMO antenna is presented to cover NR mid-band sub-6 GHz 5G wireless communication applications. The proposed antenna is designed using a microstrip feedline with 50-ohm dimensions and a rectangular patch radiator with two square cuts at the lower corner, and two rectangular slots, one at its top edge, and the other one near the bottom edge. Moreover, it has a defective ground plane to provide omnidirectional radiation pattern. In section 2, the proposed antenna's geometry evaluation steps and its design methodology is presented. In section 3, is carried out on the performance of a 4-port multi-slot MIMO antenna in terms of parametric analysis using an Ansys HFSS. Section 4 gives a complete analysis and discussion of its results and section 5 is presented with MIMO antenna diversity parameters. Finally, section 6 is presented the novelty and performance of the antenna as a conclusion followed by references.

II. DEVELOPMENT OF MULTI-SLOT MIMO ANTENNA

The section explains the evaluation process of the 4-port compact multi-slot wideband MIMO antenna along with high isolation (i.e. low coupling).

The following steps are used to design the proposed MIMO antenna is expressed below:

Stage 1: A unit antenna element of dual resonance with a wider bandwidth is designed.

Stage 2: Proposed unit antenna elements are placed at the corners of the PCB FR4 substrate using the polarization diversity technique. It shows good performance with minimum isolation among the 4-ports of MIMO antenna.

Stage 3: Furthermore, to improve the isolation among antennas a p-shaped stub is attached to the radiating element.

A. THE UNIT ELEMENT ANTENNA

A simple rectangular patch antenna is designed using four slots at various positions as illustrate in Figure 1. The performance of the proposed Multi-slot unit element antenna is studied using the Ansys HFSS tool. The rectangular patch is made with width (Wp) is 15 mm and length (Lp) is 20mm.

An FR4 substrate is used with a size of 30 mm x 20 mm x 1.6 mm (thickness i.e. h=1.6mm) with a dielectric constant of 4.4. A 50-ohm microstrip line is used to achieve better impedance matching and excite the antenna. The evaluation and schematic structure of the multi-slot unit element antenna is illustrated in Figure 2. The proposed 4-port multi-slot antenna operates from 3.60 GHz to 7.32 GHz with isolation > 15 dB. The proposed novel multi-slot antenna is capable of radiating/working in N78/79, Wi-Fi 5/6, and Vehicle2X/DSRC bands in NR mid sub-6 GHz band frequencies for 5G applications. A minimum return loss is found at -38.5 dB, and -37.1 dB at frequencies 4.18 GHz, 6.26 GHz respectively. The design equations are for the length and width of the proposed structure can be calculated from equations (1) to (6).

$$W_P = \frac{c}{2f_r\sqrt{\frac{\epsilon_r+1}{2}}} \tag{1}$$

$$L_P = \frac{c}{2f_r\sqrt{\epsilon_{reff}}} - 2\Delta L \tag{2}$$

Where,

$$L_P = L_{eff} - 2\Delta L \tag{3}$$

The effective length of the electrical length due to fringing fields can be calculated using the equations

$$L_{eff} = \frac{c}{2f_r\sqrt{\epsilon_r}} \tag{4}$$

$$\Delta L = 0.412h\frac{(\epsilon_{reff}+0.3)(\frac{W_P}{h}+0.264)}{(\epsilon_{reff}-0.258)(\frac{W_P}{h}+0.8)} \tag{5}$$

Where ϵ_{reff} effective dielectric constant and the value is calculated by

$$\epsilon_{reff} = \frac{\epsilon_r+1}{2} + \frac{\epsilon_r-1}{2}(1+12\frac{h}{w_p})^{\frac{-1}{2}}$$

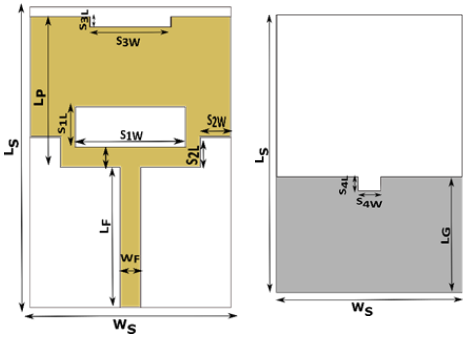

FIGURE 1. Proposed unit element antenna a) Front view b) Back view

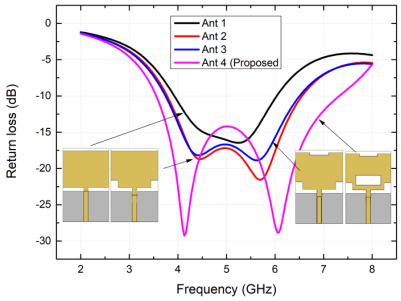

Figure 2. Evaluation of proposed multi-slot unit element antenna

Table 1 below outlines the design specifications and their associated values for the optimized unit element antenna and MIMO antenna.

TABLE 1. Multi-slot MIMO antenna design dimensions

Parameters	Value (mm)	Pameterss	Value (mm)
L_S	30	L_F	14
W_S	20	W_F	2
H_S	1.6	l_s	3.5
L_P	15	w_s	3
W_P	20	P	2
S_{1W}	11	S_{1L}	4
S_{2L}	3	S_{2W}	3
L_G	12.5	W_{SP}	56
S_{3L}	1	S_{3W}	8
S_{4L}	1.5	S_{4W}	2.4
G1	16	G2	7
P1	3	P2	2

An equivalent circuit model provides an effective means of characterizing antenna's electrical behavior by simplification their complex impedance and radiation properties into simpler terms. It consists of feed line elements L1 and R1, slot element C1, and antennas equivalent circuit R2, L2, and C2. The Lumped parameter values are calculated from [38]. An approximate model for antenna's electrical behavior can be created using a lumped element equivalent circuit model, which is simulated and optimized using AWR Design Environment. The equivalent of the unit element antenna and its simulated results are shown in Figure 3a and Figure 3b respectively.

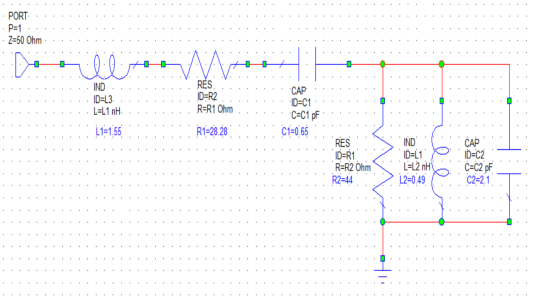

a)

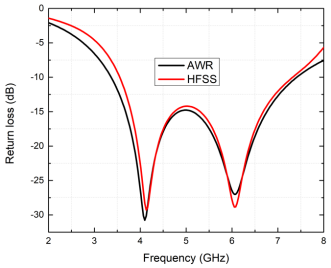

b)

Figure 3. AWR Design a) Equivalent circuit b) return loss plot

B. DESIGN OF A 4 X 4 MIMO ANTENNA

As we know, a space constraint in portable devices. Here, a 4 x 4 MIMO antenna is designed using four unit elements by placing orthogonally at the corners of the FR4 substrate with dimensions of 50 x 50 mm^2. All the single-unit element antennas are excited individually to form a 4-port MIMO antenna network. To achieve low mutual coupling among antenna ports, maintained an optimum separation between antennas less than a minimum distance of 0.5λ0. The unit element antennas are arranged orthogonally at four corners of the PCB to enhance the isolation among the 4-antenna elements, Moreover, a novel P-shaped stub is attached at the edge of radiating elements to achieve further high isolation and low mutual coupling effects. The edge-to-edge distance among nearby elements is d=7mm (0.083λ0). It is evident that a compact size MIMO antenna is proposed without degrading its performance. The proposed MIMO antenna ensures four antenna elements in two configurations.

In "Configuration 1" shows the 4-port MIMO antenna without a P-shaped and "Configuration 2" shows 4-port MIMO antenna with a P-shaped by achieving highly improved isolation between antenna ports. The proposed antenna configurations1 and configuration2 are illustrated in Figure 4a and Figure 4b respectively. The reflection coefficient (S11) and transmission coefficients (S21, S31, S41) of port1 without and with P-shaped stubs illustrated in Figure 5.

This proposed novel antenna (i.e. configuration 2) mainly covers n78/n79 bands, Wi-Fi-5/Wi-Fi6, and Vehicle2X/DSRC bands in mid sub-6 GHz band for NR 5G applications. A minimum return loss is found at -38.5 dB, and -37.1 dB at frequencies 4.18 GHz, 6.26 GHz respectively. The isolation level between antenna ports at the lower band is below -20 dB and at the higher band is -35 dB for S21 and S41 coefficients. For S31, at a lower band of almost -20dB and a higher band near -20 dB.

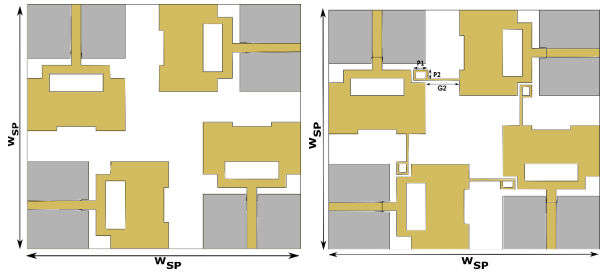

Figure 4. Proposed 4-Port MIMO antenna a) without P-stub (Ant5) b) with P-stub (Ant6)

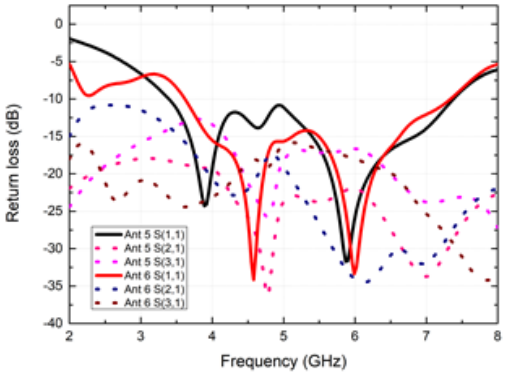

Figure 5. Return loss plot of multi-slot MIMO antenna a) without P-stub b) with P-stub

The current distribution of the proposed configuration, i.e., configuration-2 (Ant-6), was studied at two different frequencies. The antenna exhibits maximum current density around the center slot and the P-shaped stub. Port-1 is excited while the other antenna ports are terminated with a 50-ohm impedance. At 4.58 GHz, the maximum surface current density is observed at the P-shaped stub, indicating slight mutual coupling in the lower frequency band. The maximum isolation is achieved at frequencies of 4.58 GHz and 6 GHz, as depicted in Figures 6a and 6b, respectively

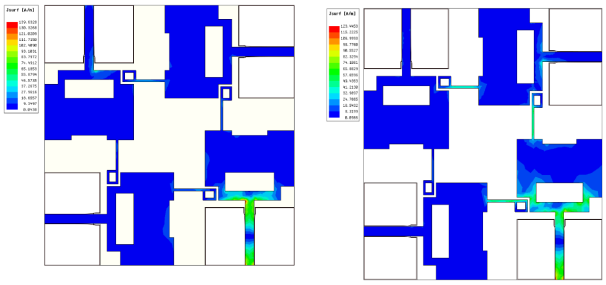

Figure 6. Surface current distribution of 4-port multi-slot antenna at a) 4.58 GHz b) 6 GHz

III. Parametric analysis

The effectiveness of the suggested antenna is primarily influenced by the dimensions of the symmetrical corner square slots and the additional slot integrated at the bottom, as illustrated in Figure 1.

In the first step, the parametric investigation of slot SL1 x SW1 involves evaluating its length, denoted as SL1, and its width, denoted as SW1. This change in SW1 length (SL1 value is kept constant) pertains to its impact on the higher frequency band of the antenna's performance. The results, as depicted in Figure 7a, demonstrate the direct influence of SL1 x SW1 length on achieving operation within the higher frequency band. Concurrently, the optimization of the width of slot SL1 x SW1, represented by SW1, is carried out by iteratively modifying its dimensions (SL1 value kept constant). This particular parameter alteration primarily drives changes in the antenna's bandwidth at the higher frequency band, as illustrated in Figure 7b. The optimized values of SL1 x SW1 are 4 mm x 11 mm.

In the second step, two symmetrical square slots are etched on the patch at the lower edge as SL2 x SW2. Furthermore, this positional variation involves displacing the slot towards the antenna's feed point and in the opposite direction. The outcomes of this observation, presented in Figure 7c, underscore the critical role of the slot's position in achieving impedance matching across both lower and higher frequency bands, providing two different current path lengths to radiate, responsible for the creation of dual resonant frequencies i.e., lower band and higher bands. The size of the two symmetrical square corner slots is optimized by varying its size 1mm x 1mm step size of 1mm as shown in the Figure 7d affects the impedance matching and disturbs the dual-band resonant. The optimized value of the SL2 x SW2 value is 3mm x 3mm. In summation, the findings from these comprehensive parametric analyses collectively contribute to a comprehensive understanding of the intricate interplay between the dimensions, width, and position of slot SL1 x SW1 in shaping the antenna's performance characteristics across different frequency bands.

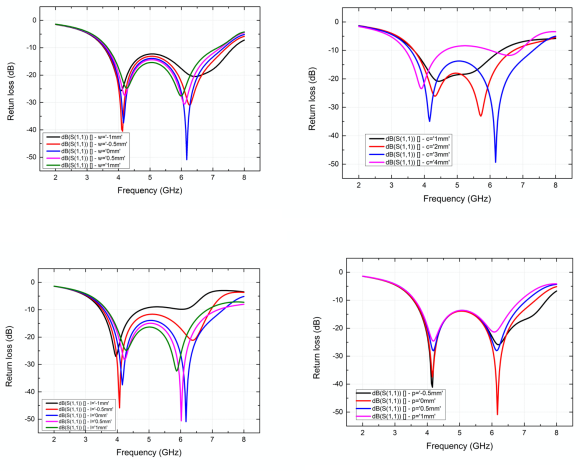

Figure7. Parametric analysis of unit element antenna

IV. RESULTS AND DISCUSSION ON PROPOSED 4-PORT MULTI-SLOT ANTENNA

The fabricated prototype of the proposed compact 4x4 multi-slot MIMO antenna is illustrated in Figure 8. Its design, analysis, and optimization have been done in FEM (Finite element Method) based High-Frequency Structural Simulator as an EM solver. The edge-mount SMA connector is used. The transmission and reflection scattering parameters of the proposed 4-port multi-slot antenna prototype results are tested by using an Anritsu (S/N: 81817008) Site Master: Model: S820E VNA and the distance between transmitting and receiving antennas is considered > $(2d^2)/\lambda_0$ in anechoic chamber as shown in Figure 9a and 9b respectively.

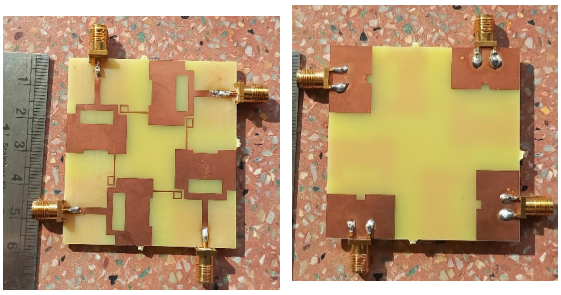

Figure 8. Fabricated prototype of 4-port multi-slot antenna a) front side b) backside

Figure 9. Measurement of proposed antenna a) return loss and isolation using VNA setup b) Radiation Patten measurement

A. RETURN LOSS

Figure 10 represents simulated and measured results of the proposed MIMO antenna S-parameter transmission and reflection coefficients. One of the ports (i.e. Port-1) is fed and the remaining ports of the antenna are terminated by a 50-ohm impedance load. Here, the simulated and measured results are almost overlapped over entire impedance bandwidth. However, a slight deviation occurred in simulated and measured results probably due to radiating losses, dielectric loss, and ohmic loss. The proposed 4-port multi-slot MIMO antenna system operates from 3.60 GHz – 7.33 GHz. Moreover, its bandwidth, isolation, and impedance matching are achieved within a compact-size antenna without degrading its performance. This antenna can effectively work for the n78 (3.3 –3.8 GHz) band, n79 (4.4 –5 GHz) band, Wi-Fi-5 (5.15 - 5.85 GHz) band, Vehicle2X/DSRC (5.85 GHz - 5.90 GHz) band, and Wi-Fi-6 (5.925 - 7.125 GHz) band in mid-NR sub-6 GHz for 5G applications.

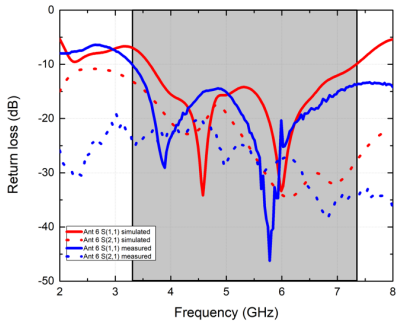

Figure 10. Simulated and measured results of the proposed MIMO antenna

B. RADIATION PATTERNS

Figure 9b shows the arrangement and setup of the proposed antenna prototype in an anechoic chamber. Moreover, the simulated and measured (2D) radiation characteristics are studied. These radiation characteristics are analyzed in the E-plane in XY (at $\Phi=0^0$) and H-plane in YZ planes (at $\Phi=90^0$) at 4.2 GHz, and 5.8 GHz respectively. To understand the stability of radiation intensity of the 4-port multi-slot antenna in terms of major lobes, minor lobes, and null directions are studied. The minimal measured results are deviated from simulated results due to density variation in soldering material or measurement errors. The characteristics of the radiation are stable and better results in the sub 6GHz band as illustrated in Figure 11.

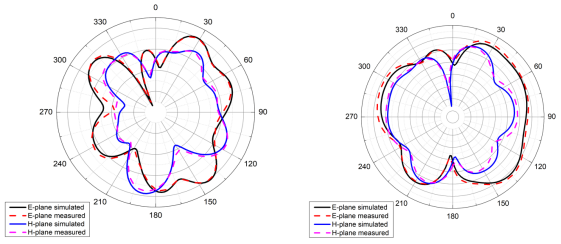

Figure 11. The 2D radiation patterns of the 4-port multi-slot antenna at a) 4.2 GHz b) 5.8 GHz

C. GAIN AND EFFICIENCY

The proposed 4-port multi-slot antenna's realized gain and radiation efficiency plot has been illustrated in Figure 12. It is observed that the gain varied from 3.3 dB-5.5 dB over the operating frequency band 4.6 GHz-7.125 GHz with an average peak gain of 4.5 dB. The maximum peak gain of 5.2 dB is observed at 6 GHz for the antenna. The radiation efficiency plotted from 4.6 GHz-7.125 GHz, the average efficiency of the antenna is 95%.

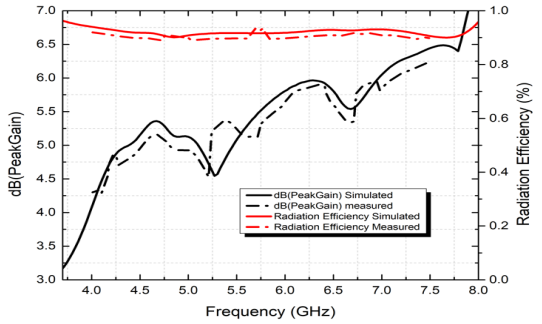

Figure 12. The peak gain, and efficiency plot

V. PERFORMANCE DIVERSITY METRICS OF MULTI-SLOT MIMO ANTENNA

The MIMO antenna system is tested with antenna diversity parameters like ECC, CCL, etc, along with conventional antenna parameters.

A. ENVELOPE CORRELATION COEFFICIENT

The ECC measures the correlation between/among antenna elements to show how radiation patterns are independent. Therefore, the ECC indicates the interference level between antenna elements. To maintain the stable performance of the MIMO antenna, its value should be 0.5. Here, the ECC parameter is expressed and calculated with S-parameters using equation 7 below,

$$\rho = \frac{|S_{11}^{*}S_{12}+S_{21}^{*}S_{22}|^2}{(1-|S_{11}|^2-|S_{21}|^2)(1-|S_{12}|^2-|S_{22}|^2)} \quad (7)$$

Here S_{11} and S_{22} are return loss S-parameters and S_{21} and S_{12} are isolation S-parameters

The ECC simulated and measured are within the limit as illustrated in Figure 13a. The measured ECC value is below 0.004 in the sub-6 band.

B. CHANNEL CAPACITY LOSS

The channel capacity indicates the capability of a channel without a significant loss when the maximum information rate can pass through the channel. The CCL parameter is expressed and calculated by the below equations 8,

$$C_{loss} = -log_2^{|\Psi^R|} \quad (8)$$

Here, $\Psi^R = \Psi\lfloor\Psi_{xy}\rfloor, (x,y) \in (1,2,3,4)$ represents a correlation matrix while EM waves receiving at receiving antenna, with

$$\Psi_{xy} = 1 - |S_{ii}|^2 - |S_{ij}|^2 \quad (9)$$

$$\Psi_{xy} = 1 - |S_{ji}|^2 - |S_{jj}|^2 \quad (10)$$

$$\Psi_{xy} = -(S_{ii}^{*}S_{ij} + S_{ji}^{*}S_{jj}) \quad (11)$$

$$\Psi_{xy} = -(S_{ij}^{*}S_{ii} + S_{jj}^{*}S_{ji}) \quad (12)$$

For the CCL value below 0.4 bps/Hz will be considered as better performance in the MIMO antenna system. For this multi-slot MIMO antenna, the CCL parameter value is below 0.14 bps/Hz over the entire sub-6 band. Figure 13b shows simulated and measured CCL plot of the proposed antenna.

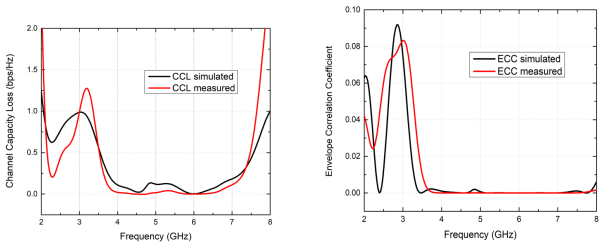

FIGURE 13. The 4-port multi-slot MIMO antenna diversity parameters plots a) ECC and b) CCL

VI. Comparison of multi-slot MIMO antenna with other existing MIMO antennas:

In literature, various decoupling networks/structures/techniques are proposed to prove high isolation among the multiple ports in sub-6 GHz 5G wireless applications. In this paper a novel compact 4 x 4 Multi-slot MIMO antenna for 5G N78/79, Wi-Fi 5/6, and Vehicle2X/DSRC frequency bands in mid 5G Sub-6 GHz. Moreover, the port multi-band antenna has a high directivity, isolation, and antenna efficiency in the NR 5G sub-6 GHz band. Table 2 illustrates the advantages in terms of various parameters to express the novelty of the proposed 4-port multi-slot antenna with other existing MIMO antennas.

TABLE 2. Comparison of 4-port multi-slot MIMO antenna with other existing MIMO antennas

Ref	Dimensions, Substrate (ε_r)	Bands	MIMO Diversity Parameters			Gain (dB), Efficiency	Isolation Technique
			Isolation	ECC	CCL		
In this article	56 x 56 x 1.6	3.6 – 7.34	>-18	0.004	0.14	5.295	P-shape stub
[3]	70.5 x 83 x 1.6 FR4 (4.4)	2.4–2.52, 3.66–4, 4.62–5.52	-18.5	0.001	0.4	1 85	Orientation
[4]	30 x 30 x 0.8 FR4 (4.4)	4.58 - 6.12	15.4	0.15	NA	4.0267-82	Parasitic elements
[5]	65 × 65 × 1.6 FR4 (4.1)	4.95 - 5.35	>-22	<0.15	0.18	6 -	Shorting walls
[7]	60x60x 0.8 FR4 (4.4)	2.4-2.485 3.4-3.6	24	0.007	NA	3.45 -	Parasitic elements
[9]	50x50x 1.6 FR4 (4.4)	4.30 - 6.45	-20	0.004	NA	5.5 -	Orientation
[11]	72x72x FR4	2.34 - 2.56	10	0.01	NA	2 79-92	Diagonal Parasitic elements
[12]	75x75	4.96 –5.5	10	<0.03		5.563	No isolation Technique
[17]	62x25.6x1.524 Rogers RO4003 (3.55)	3.05 - 3.62 4.62 - 4.99	-16	<0.002	<0.32	3.8485	Defected ground with L-shaped slot with strip
[19]	43x35.5 FR4 (4.4)	5.6-5.95	-22	0.0001	NA	- 85	No isolation technique
[22]	66x66x 1.6 FR4 (4.3)	2.3-2.7	17	0.04	0.6	3.7 -	Cross-shaped stub and the ring-shaped stripes

NA- Not Available in the reference

VII. CONCLUSION

A novel compact 4 x 4 Multi-slot antenna for N78/79, Wi-Fi 5/6, and V2X/DSRC applications in mid-band Sub-6 GHz band for NR 5G communication is proposed, and its performance is discussed in this paper. Initially, the performance of a 2-port multi-slot antenna performance is observed in terms of orientation/direction to improve the isolation between antenna ports. Further, a 4x4 antenna system is proposed using a single antenna by rotating 90^0 at the corners of the FR4 PCB. Finally, the p-stub is attached to a 4x4 multi-slot antenna to improve impedance matching and isolation. The 4-port multi-slot MIMO antenna operates in a frequency band ranging from 3.60 GHz – to 7.33 GHz. The prototype tested and HFSS simulated results are almost similar. Moreover, the 4-port multi-slot antenna has stable radiation patterns in elevation and azimuth planes, high radiation efficiency, and high gain. The MIMO antenna diversity CCL, and ECC parameters are studied. This antenna performance can be envisaged for N78/79, Wi-Fi 5/6, and Vehicle2X/DSRC bands for 5G applications in the mid sub-6 GHz frequency band.

REFERENCES

[1] R. Subhanrao Bhadade and S. Padmakar Mahajan, "'Circularly polarized 4 × 4 MIMO antenna for WLAN applications,'" *Electromagnetics*, vol. 39, no. 5, pp. 325–342, 2019, doi: 10.1080/02726343.2019.1619227.

[2] R. Yang, S. Xi, Q. Cai, Z. Chen, X. Wang, and G. Liu, "A compact planar dual-band multiple-input and multiple-output antenna with high isolation for 5g and 4g applications," *Micromachines*, vol. 12, no. 5, pp. 2–9, 2021, doi: 10.3390/mi12050544.

[3] D. Dileepan, S. Natarajan, and R. Rajkumar, "A high isolation multiband mimo antenna without decoupling structure for wlan/wimax/5g applications," *Prog. Electromagn. Res. C*, vol. 112, no. March, pp. 207–219, 2021, doi: 10.2528/PIERC21032605.

[4] M. Yang and J. Zhou, "A compact pattern diversity MIMO antenna with enhanced bandwidth and high-isolation characteristics for WLAN/5G/WiFi applications," *Microw. Opt. Technol. Lett.*, vol. 62, no. 6, pp. 2353–2364, 2020, doi: 10.1002/mop.32334.

[5] V. Sharma, M. D. Upadhayay, A. V. Singh, and J. Prajapati, "Hammer-shaped element-based compact mimo antenna for wlan application," *Prog. Electromagn. Res. Lett.*, vol. 97, no. March, pp. 121–130, 2021, doi: 10.2528/PIERL21031604.

[6] J. Kulkarni, A. Desai, and C. Y. D. Sim, "Two port CPW-fed MIMO antenna with wide bandwidth and high isolation for future wireless applications," *Int. J. RF Microw. Comput. Eng.*, vol. 31, no. 8, 2021, doi: 10.1002/mmce.22700.

[7] W. A. E. Ali, M. I. Ashraf, and M. A. Salamin, "A dual-mode double-sided 4 × 4 MIMO slot antenna with distinct isolation for WLAN/WiMAX applications," *Microsyst. Technol.*, vol. 27, no. 3, pp. 967–983, 2021, doi: 10.1007/s00542-020-04984-6.

[8] J. Kulkarni, A. Desai, and C. Y. D. Sim, "Wideband Four-Port MIMO antenna array with high isolation for future wireless systems," *AEU - Int. J. Electron. Commun.*, vol. 128, p. 153507, 2021, doi: 10.1016/j.aeue.2020.153507.

[9] A. W. Mohammad Saadh *et al.*, "A compact four-element MIMO antenna for WLAN/WiMAX/satellite applications," *Int. J. Commun. Syst.*, vol. 33, no. 14, pp. 1–17, 2020, doi: 10.1002/dac.4506.

[10] R. Krishnamoorthy, A. Desai, R. Patel, and A. Grover, "4 Element compact triple band MIMO antenna for sub-6 GHz 5G wireless applications," *Wirel. Networks*, vol. 27, no. 6, pp. 3747–3759, 2021, doi: 10.1007/s11276-021-02734-8.

[11] S. Chouhan, D. K. Panda, and V. S. Kushwah, "Modified circular common element four-port multiple-input-multiple-output antenna using diagonal parasitic element," *Int. J. RF Microw. Comput. Eng.*, vol. 29, no. 2, 2019, doi: 10.1002/mmce.21527.

[12] L. Malviya and S. Chouhan, "Multi-cut four-port shared radiator with stepped ground and diversity effects for WLAN application," *Int. J. Microw. Wirel. Technol.*, vol. 11, no. 10, pp. 1044–1053, 2019, doi: 10.1017/S1759078719000680.

[13] P. Pradeep, K. J. Sankar, and P. C. Sekhar, "A Compact Semi - circular Slot MIMO Antenna with Enhanced Isolation for Sub - 6 GHz 5G WLAN Applications," *Wirel. Pers. Commun.*, no. 0123456789, 2022, doi: 10.1007/s11277-022-09730-x.

[14] G. Naga Jyothi Sree and S. Nelaturi, "Design and experimental verification of fractal based MIMO antenna for lower sub 6-GHz 5G applications," *AEU - Int. J. Electron. Commun.*, vol. 137, no. February, p. 153797, 2021, doi: 10.1016/j.aeue.2021.153797.

[15] N. B. Slits, J. Li, Q. Chu, S. Member, and T. Huang, "A Compact Wideband MIMO Antenna With Two," *IEEE Trans. Antennas Propag.*, vol. 60, no. 2, pp. 482–489, 2012.

[16] M. M. Hasan *et al.*, "Gain and isolation enhancement of a wideband MIMO antenna using metasurface for 5G sub-6 GHz communication systems," *Sci. Rep.*, vol. 12, no. 1, pp. 1–17, 2022, doi: 10.1038/s41598-022-13522-5.

[17] P. Sharma, R. N. Tiwari, P. Singh, and B. Kumar, "International Journal of Electronics and Communications Dual-band trident shaped MIMO antenna with novel ground plane for 5G applications," *AEUE - Int. J. Electron. Commun.*, vol. 155, no. August, p. 154364, 2022, doi: 10.1016/j.aeue.2022.154364.

[18] A. M. Ibrahim, I. M. Ibrahim, and N. A. Shairi, "Compact MIMO antenna with high isolation for 5G smartphone applications," *J. Eng. Sci. Technol. Rev.*, vol. 12, no. 6, pp. 121–125, 2019, doi: 10.25103/jestr.126.15.

[19] K. Malaisamy, M. Santhi, and S. Robinson, "Design and analysis of 4 × 4 MIMO antenna with DGS for WLAN applications," *Int. J. Microw. Wirel. Technol.*, vol. 13, no. 9, pp. 979–985, 2021, doi: 10.1017/S1759078720001658.

[20] S. S. Jehangir and M. S. Sharawi, "A Miniaturized UWB Biplanar Yagi-Like MIMO Antenna System," *IEEE Antennas Wirel. Propag. Lett.*, vol. 16, no. c, pp. 2320–2323, 2017, doi: 10.1109/LAWP.2017.2716963.

[21] N. K. Gollamudi, Y. V Narayana, and A. M. Prasad, "A Novel Cow-Head Shaped Multiple Input Multiple Output Antenna for 5G Sub : 6 GHz N77 / N78 & N79 Bands Applications," vol. 122, no. July, pp. 83–93, 2022.

[22] A. A. Yussuf and S. Paker, "Design of a compact quad-radiating element MIMO antenna for LTE/Wi-Fi application," *AEU - Int. J. Electron. Commun.*, vol. 111, p. 152893, 2019, doi: 10.1016/j.aeue.2019.152893.

[23] M. H. Reddy, D. Sheela, and A. Swaminath, "A four port circularly polarized printed multiple-input multiple-output antenna with enhanced isolation," *Int. J. Commun. Syst.*, vol. 35, no. 4, 2022, doi: 10.1002/dac.5061.

[24] S.- Ghz *et al.*, "A Compact MIMO Antenna with Improved Isolation for ISM ," pp. 1–10, 2022.

[25] K. V. Babu, S. Das, S. Lakrit, S. K. Patel, B. T. P. Madhav, and H. Medkour, "Compact Dual-Band Printed MIMO Antenna with Very Low Mutual Coupling for WLAN, Wi-MAX, Sub-6 GHz 5G and X-Band Satellite Communication Applications," *Prog. Electromagn. Res. C*, vol. 117, pp. 99–114, 2021, doi: 10.2528/PIERC21100201.

[26] Malathi, A. C. J., Reddy, B. V. K., & Phanindra, K. R. (2024). A Decoupling method using Split Ring Resonator (SRR) for Tri-band MIMO Antenna for WLAN LTE Band and 5G applications. *Advanced Electromagnetics*,*13*(1),19–24.https://doi.org/10.7716/aem.v13i1.227

[27] Mohapatra, S., Das, S., Panda, J. R., Sahu, S., & Raghavan, S. (2024). Dual band Orthogonal Polarized 2-port MIMO Antenna for Cognitive Radio Applications. Advanced Electromagnetics, 13(1), 1–8. https://doi.org/10.7716/aem.v13i1.2164.

[28] Hussain, N.; Pham, T.D.;Tran, H.-H. Circularly Polarized MIMO Antenna with Wideband and High Isolation Characteristics for C-Band Communication Systems. Micromachines 2022, 13, 1894. https://doi.org/10.3390/mi13111894.

[29] Kiouach, F., El Ghzaoui, M., Das, S. et al. A Compact Wideband Printed 4 × 4 MIMO Antenna with High Gain and Circular Polarization Characteristics for mm-wave 5G NR n260 Applications. Wireless Pers Commun 133, 1857–1886 (2023). https://doi.org/10.1007/s11277-023-10850-1.

[30] Khan, I.;Wu, Q.; Ullah, I.; Rahman, S.U.; Ullah, H.; Zhang, K. Designed Circularly Polarized Two-Port Microstrip MIMO Antenna for WLAN Applications. Appl.Sci.2022,12,1068.https://doi.org/10.3390/app12031068.

[31] F. Bilotti, A. Toscano, L. Vegni, K. Aydin, K. B. Alici and E. Ozbay, "Equivalent-Circuit Models for the Design of Metamaterials Based on Artificial Magnetic Inclusions," in *IEEE Transactions on Microwave Theory and Techniques*, vol. 55, no. 12, pp. 2865-2873, Dec. 2007, doi: 10.1109/TMTT.2007.909611.